

AD-A262 280



Form Approved
GSA No. 0704-0188

and the Office of Management and Budget, a Federal Acquisition Project (FPA) 4-100, Washington, DC 20548.

1. REPORT TYPE AND DATES COVERED
Annual Technical 1 Sep 91 - 14 Oct 92

61102F
AFOSK-90-0339
2309
AS

Dr Robert King

Massachusetts Institute of Technology
Dept of Earth, Atmospheric, and Planetary Sciences
Cambridge MA 02139-4307

AFOSR-TR-

Dr Dickinson
AFOSR/NL
110 Duncan Avenue, Suite B115
Bolling AFB DC 20332-6448

18. SPONSORING / MONITORED
AGENCY REPORT NUMBERS

11. SUPPLEMENTARY NOTES

12a. DISTRIBUTION/AVAILABILITY STATEMENT

Approved for public release; distribution unlimited

126. SUBSTITUTION CASE

ABSTRACT (Maximum 200 words)

Recent geological and geodetic studies have suggested that the region surrounding Vandenberg AFB is undergoing active crustal deformation, with important implications for both the geodetic stability and the seismogenic potential of the Western Test Range (WTR) (Feigl *et al.*, 1990). Part of the evidence for significant deformation was obtained from GPS measurements over a broad area of central and southern California, which we carried out in cooperation with other university and government scientists from 1987 through 1991. Although useful in defining the regional tectonic setting, these measurements are of insufficient spatial and temporal density to answer many important questions about the seismogenic potential of Vandenberg. The sites observed in the March 1992 survey are given in Table 1, and a map of the enlarged network is shown in Figure 1. Four new sites (CASM, FAARF, RDRK, and FIGP) were established on or bridging three of the four major anticlines that cut the Santa Maria Basin. Our primary scientific goal is to localize the measured deformation on one or more of these structures. One of the new sites (SOAP) provides a more stable anchor for that part of our network south of the Santa Ynez River Fault. Three other sites occupied for the first time (ARG3, VINA, VANP), as well as two previously occupied (ALVA, VNDN), are existing DMA sites near the south Base PGGG site (VNDP). This small sub-network provides a means to monitor the local stability of the three sites (VAND, VNDN, and VNDP) that have been or will be used for long-term monitoring of deformation. The two-day occupation of the South Base sub-network also provided us the opportunity to study more carefully the effects of atmospheric water vapor on GPS measurements.

14. SUBJECT TERMS

12. NUMBER OF PAGES

93 9 31 050

IS ANY GOOD?

17. SECURITY CLASSIFICATION
OF REPORT
(U)

18. SECURITY CLASSIFICATION
OF THIS PAGE
(U)

19. SECURITY CLASSIFICATION
OF ABSTRACT
(U)

24. LIMITATION OF ABSTRACT

(U)

**Crustal Deformation Measurements in the Vicinity of
Vandenberg Air Force Base**

**Grant AFOSR-90-0339
(MIT OSP No. 75390)**

**Annual Technical Report
for the period
1 September 1991 - 14 October 1992**

**Submitted to
Air Force Office of Scientific Research**

**Stanley Dickinson
Program Manager
AFOSR/NL Bolling AFB, DC 20332-6448**

**Vernita J. Slater
Contracting Officer
AFOSR/PKZA
Bolling AFB, DC 20332-6448**

by

DTIC QUALITY INSPECTED 4

**Robert W. King
Principal Investigator
Department of Earth, Atmospheric, and Planetary Sciences
Massachusetts Institute of Technology
Cambridge, MA 02139**

22 February 1993

Accession For	
NTIS CRA&I	<input checked="checked" type="checkbox"/>
DTIC TAB	<input type="checkbox"/>
Unannounced	<input type="checkbox"/>
Justification	
By	
Distribution /	
Availability Codes	
Dist	Avail and/or Special
A-1	

INTRODUCTION

Recent geological and geodetic studies have suggested that the region surrounding Vandenberg AFB is undergoing active crustal deformation, with important implications for both the geodetic stability and the seismogenic potential of the Western Test Range (WTR) [Feigl *et al.*, 1990]. Part of the evidence for significant deformation was obtained from GPS measurements over a broad area of central and southern California, which we carried out in cooperation with other university and government scientists from 1987 through 1991. Although useful in defining the regional tectonic setting, these measurements are of insufficient spatial and temporal density to answer many important questions about the seismogenic potential of Vandenberg.

In 1989 we received funding from AFOSR under the Commander's Reserve Fund (Grant AFOSR-89-0400), with matching funds from MIT, to purchase five GPS receivers and to begin a series of measurements designed to determine the magnitude and spatial distribution of deformation in the Santa Maria Fold and Thrust Belt (SMFTB), a region encompassing the major faults and folds within 50 km of Vandenberg. Two additional receivers were purchased in May 1992 and have since been installed in continuously operating GPS stations at Vandenberg and the China Lake Naval Weapons Center. They are operated as part of the Permanent GPS Geodetic Array (PGGA) in California, providing the ability to monitor not only interseismic deformation, but any transient motion which might occur prior to, during, or after an earthquake.

The pre-grant studies of Vandenberg tectonics and our progress during the first year of this grant have been completely described in the doctoral thesis of Kurt L. Feigl, completed at M. I. T. in September 1991 and submitted with last year's annual report.

GPS MEASUREMENTS

Since February 1990, we have carried out five GPS surveys involving the stations of the Vandenberg network. Three of these surveys (February and September 1990, and March 1992) included most or all of the current network; the other two (March 1990 and February 1991) included two or three Vandenberg stations as part of a remeasurement of the regional central and southern California networks. The details of the first four surveys are given in Chapter 4 of Feigl [1991], especially Figures 4.1–4.3, Tables 4.1–4.6, and the text on pp. 124–125 and 137. In the fifth survey (March 1992) we remeasured the relative positions of eight of the Vandenberg-network stations surveyed in 1990, and also established nine new stations to densify the network.

The sites observed in the March 1992 survey are given in Table 1, and a map of the enlarged network is shown in Figure 1. Four new sites (CASM, FARF, RDRK, and FIGP) were established on or bridging three of the four major anticlines that cut the Santa Maria Basin. Our primary scientific goal is to localize the measured deformation on one or

more of these structures. One of the new sites (SOAP) provides a more stable anchor for that part of our network south of the Santa Ynez River Fault. Three other sites occupied for the first time (ARG3, VINA, VANP), as well as two previously occupied (ALVA, VNDN), are existing DMA sites near the South Base PGGA site (VNDP). This small subnetwork provides a means to monitor the local stability of the three sites (VAND, VNDN, and VNDP) that have been or will be used for long-term monitoring of deformation.

The two-day occupation of the South Base subnetwork also provided us the opportunity to study more carefully the effects of atmospheric water vapor on GPS measurements. Vandenberg is a promising setting for this study since it is subjected to strong atmospheric gradients from the onshore winds. Both very long baseline interferometry (VLBI) and GPS observations conducted there over the past decade show atmospheric errors that are greater than those for many other sites in California sites. Our study is further enhanced by the availability of radiosonde data obtained twice daily by the base weather detachment. Although the detachment normally alternates launches between North and South Vandenberg, during the period of our observations they altered their schedule to take all the measurements from South base.

Table 1. Observations acquired during the March 1992 survey

		----- Receiver -----					
Mar	day	day	MIT1	MIT2	MIT3	MIT4	CIT1 CIT2
Mon	2	062	ALAM	----	----	----	VAND VNDN
Tue	3	063	ALAM	----	GRAS	LIND	VAND VNDN
Wed	4	064	LOSP	----	GRAS	LIND	VNDP VNDN
Thu	5	065	LOSP	----	GRAS	LIND	VNDPa VNDNa
Fri	6	066	LOSP	----	FIGP	----	----a ----a
Sat	7	067	FARF	DMAV	FIGP	MADC	VNDPa ----a
Sun	8	068	FARF	VNDN	VINA	MADC	VNDP SOAP
Mon	9	069	RUS1	3ARG	VINA	ALVA	VNDP SOAP
Tue	10	070	RUS1	3ARG	VINA	ALVA	VNDP SOAP
Wed	11	071	----	----	VINA	----	VNDP ----
Thu	12	072	LIND	DMAV	RDRK	----	VNDP VNDN
Fri	13	073	LIND	DMAV	RDRK	CASM	VNDP VNDN
Sat	14	074	LIND	ALAM	RDRK	CASM	VNDP GRAS
Sun	15	075	LIND	ALAM	----	CASM	VNDP GRAS
tot			13	8	12	12	10 10 64
						2a	1

Days 069 and 070 constitute the "atmospheric experiment".

a = cow attack

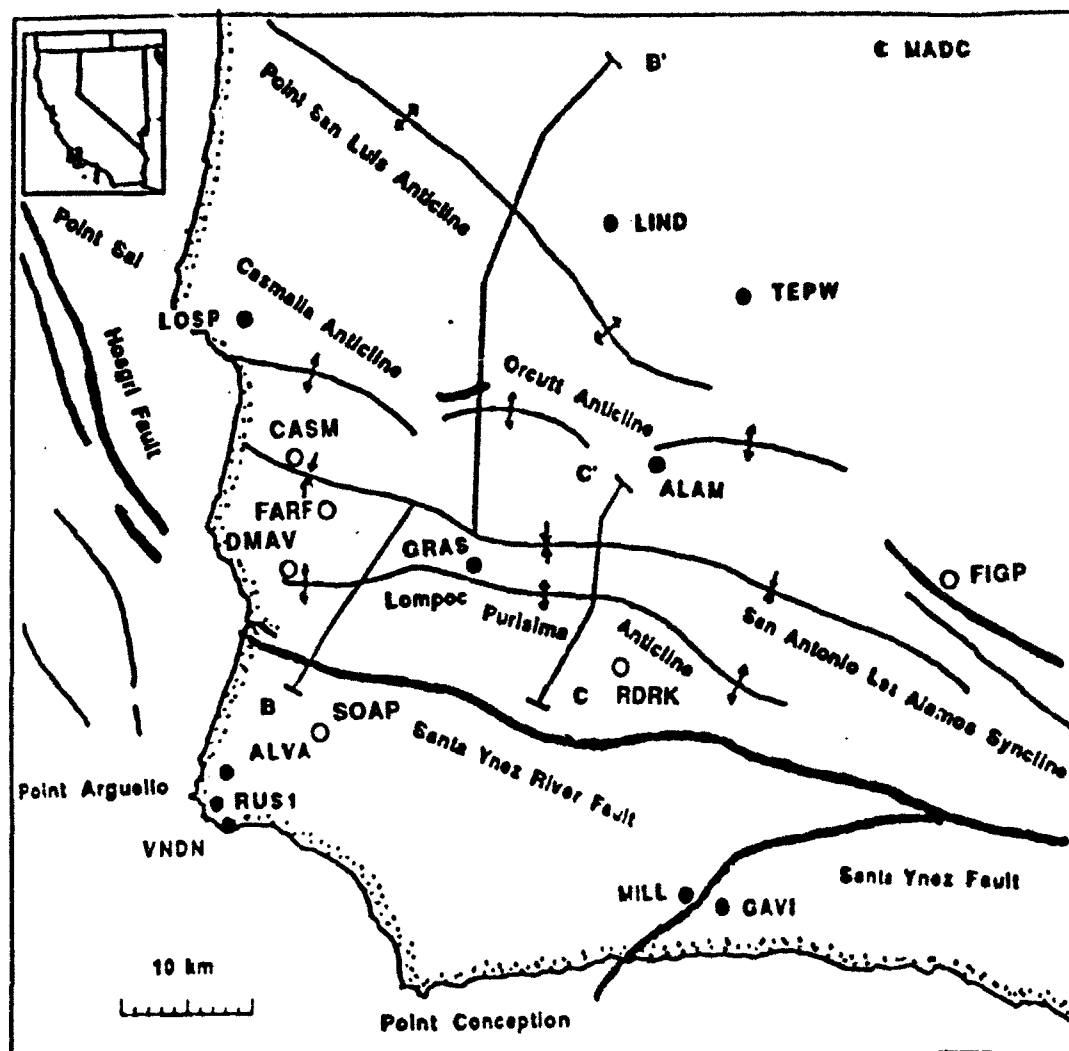


Figure 1. Tectonic map of Vandenberg and vicinity (Santa Maria Fold and Thrust Belt) showing the location of faults (thick lines) and folds (thin lines) and of the GPS stations (dots with 4-letter codes) included in our study. Solid dots indicate stations which have been surveyed both in 1990 and 1992; open dots indicate stations surveyed for the first time in 1992. Only three of the seven stations in the dense South Base network near Point Arguello are shown.

DATA ANALYSIS

GPS observations in the vicinity of Vandenberg cannot be understood in isolation from the rest of southern California. Only by determining (vector) motions of the stations in the Vandenberg network relative to stations outside the network can we assess the relative importance of dilatation and rotation in the pattern of deformation. Moreover, it is essential to include in the analysis observations from a continental- or global-scale network in order to reduce the errors due to unmodeled motions of the GPS satellites. Thus, we have analyzed all of the Vandenberg data simultaneously with both GPS and VLBI data from central and southern California and a global network of stations. Much of our effort during the past year has been spent in refining this analysis and describing it in a comprehensive paper submitted in December to the *Journal of Geophysical Research* [Feigl *et al.*, 1992]. Figure 2 shows our estimates of the velocities of 35 sites in central and southern California. The dominant motion at this scale is the simple shear due to the San Andreas Fault (SAF) system, which contributes a few millimeters per year even to sites as far west as Vandenberg.

In order to understand better more local sources of deformation, we show in Figure 3 residual velocities after removing an approximate model of velocities associated with the SAF. Of the five stations in the Santa Maria Fold and Thrust Belt (SMFTB), Mount Lospe (LOSP) and Madre (MADC) exhibit residual motions significantly different from zero at 95% confidence. In particular, the residual velocity of Madre with respect to the Vandenberg South Base site (VNDN) implies 1.8 ± 0.9 mm/yr of shortening and 2.9 ± 0.9 mm/yr of right-lateral slip in the frame defined by the local (N60°W) strike of the folds.

The rate of shortening is compatible with the geological rate of 2–5 mm/yr estimated from a balanced cross section [Namson and Davis, 1990], but smaller than the 6 ± 1 mm/yr estimated from our earlier comparison of GPS and historical survey data [Feigl *et al.*, 1990]. The latter study, however, assumed uniform strain in the SMFTB, no net rotation, and no strain accumulating from the locked SAF. All three of these hypotheses are suspect in light of the spatially varying strain rates and the suggestion of rotation from our analysis of the larger California network, and of our model calculation of 3 mm/yr of relative motion between Vandenberg and Madre.

The amount of right-lateral strike-slip shear in the SMFTB is larger than expected, given the lack of faults active in the Quaternary [Jennings, 1975; Sylvester and Darrow, 1979; Clark *et al.*, 1984]. One explanation would be unmodeled strain accumulation on the SAF. Alternatively, strain accumulation on the offshore Hosgri fault [Hall, 1987; 1981] may be indicated. The addition of data from the March, 1992, survey and the continuous observations from the Vandenberg PPGA site should help to distinguish among these hypotheses.

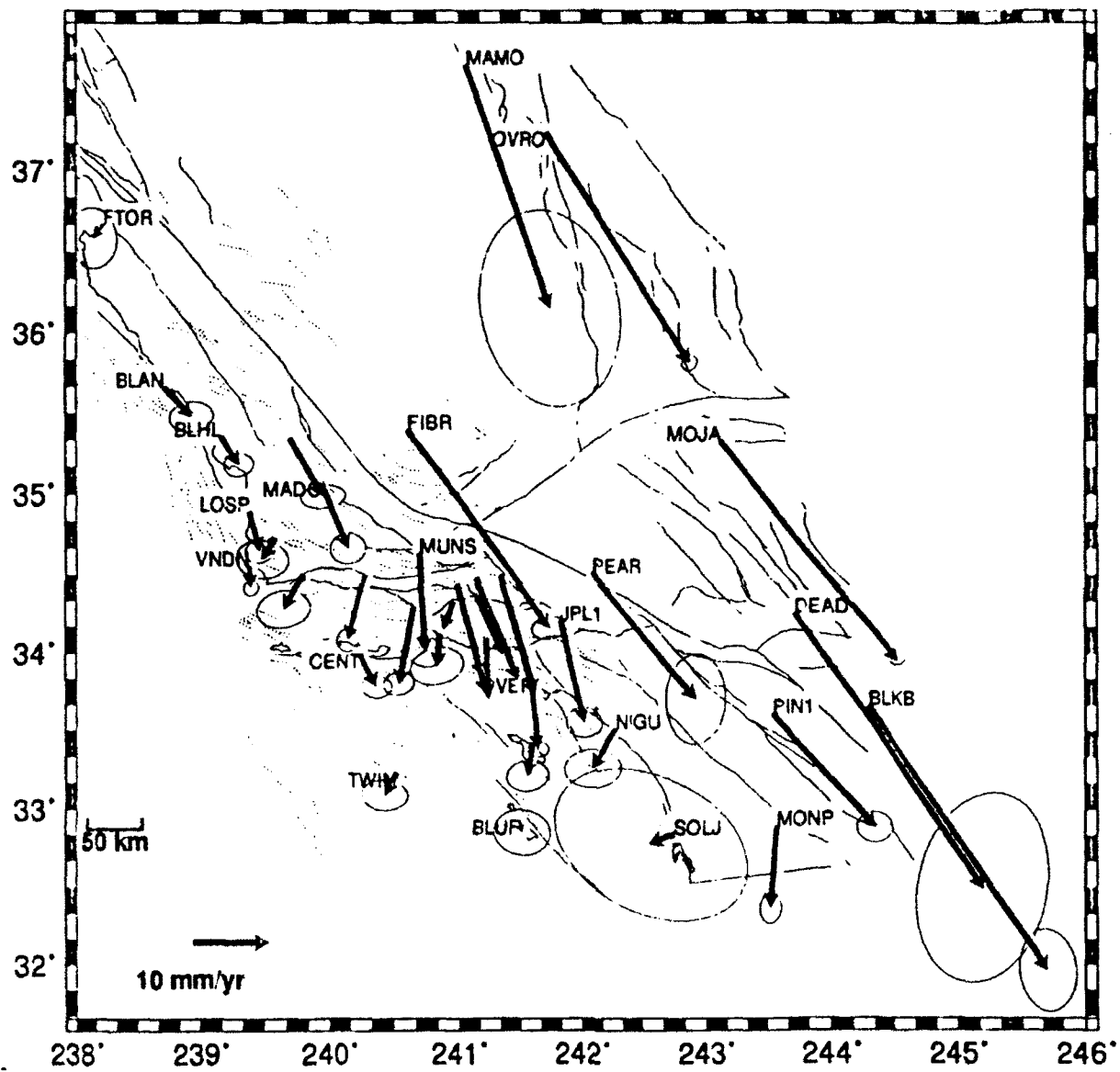


Figure 2. Estimated velocity of central and southern California stations relative to the Pacific plate, from Feigl *et al.* [1992]. The ellipses denote the region of 95% confidence.

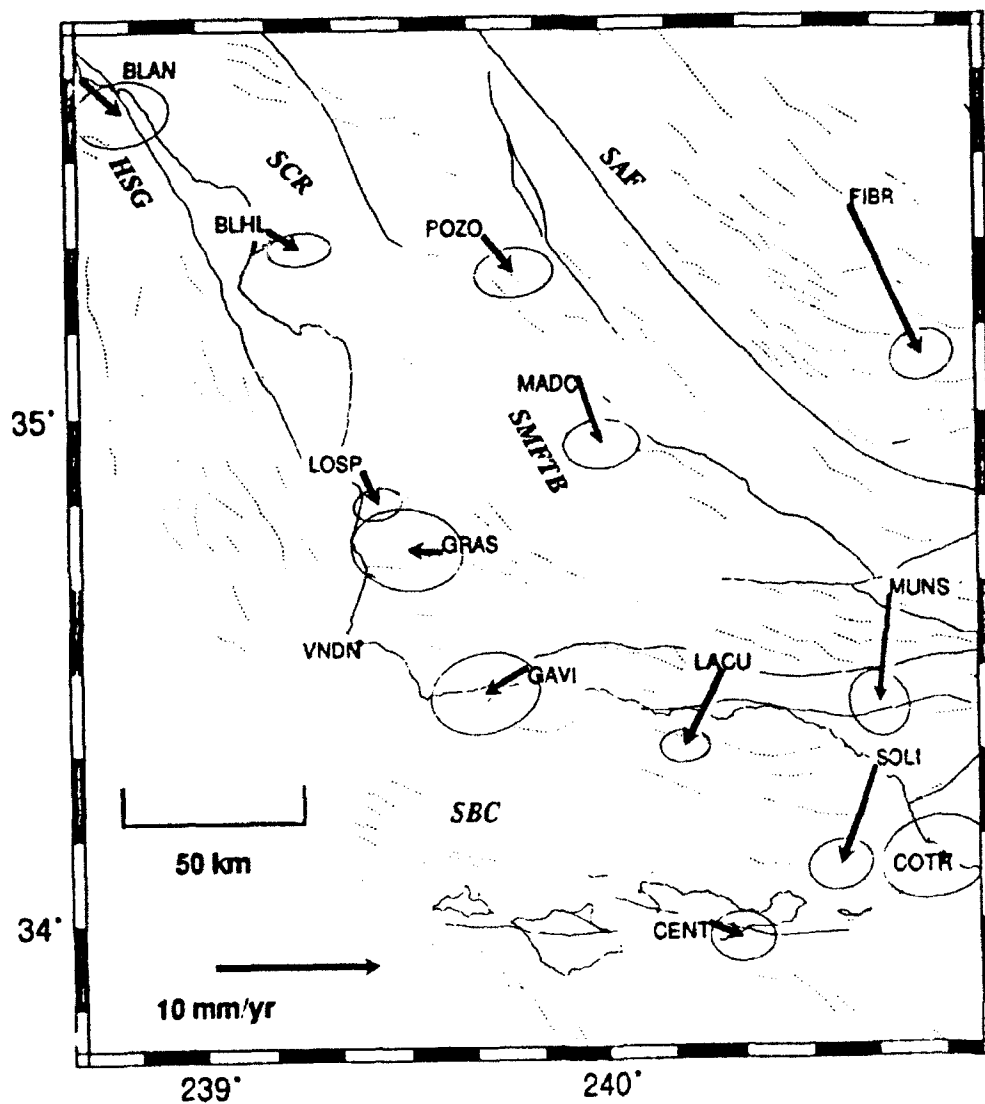


Figure 3. Residual velocities with respect to Vandenberg (VNDN) after removal of a model of shear strain due to the San Andreas fault system, from *Feigl et al.* [1992]. Note that the velocity scale is double that of the previous figure. The tectonic features include the San Andreas fault (SAF), the Santa Barbara Channel (SBC), and the southern Coast Ranges (SCR).

An unexpected result from the Vandenberg PGGA station has been the contribution of its observations to geodetic determination of far-field displacements from the Landers (M_w 7.3) and Big Bear (M_w 6.2) earthquakes of 28 June 1992. These earthquakes occurred within 100 km of the PGGA sites at Pinyon Flat Observatory (PIN1), operated by the University of California at San Diego, and the NASA Goldstone Complex (GOLD) (Figure 4). These two sites, plus the PGGA sites at Scripps (SIO2) and the Jet Propulsion Laboratory in Pasadena (JPLM), were displaced by more than a centimeter by the earthquakes. Our analysis of these data, in collaboration with our colleagues at Scripps, has been reported in a letter to *Nature* published this month and attached to this report [Bock *et al.*, 1993]. A supplemental plot of the Vandenberg displacements, not included in the *Nature* letter, is shown in Figure 5. There is a hint of a displacement of a few millimeters in both the north and east component of the Vandenberg position. The north displacement, estimated formally to be 4.5 ± 1.6 mm, is significantly larger than the value (0.9 mm) predicted by our model. An analysis of the Vandenberg observations over a longer period of time will be necessary to determine if the uncertainty in our estimated displacement is realistic. Note also in Figure 5 the large (>50 mm) systematic signature in the vertical position of Vandenberg. We believe that this is due to deficiencies in our models for satellite-orbit and atmospheric effects. The long series of PGGA observations provide an important data set for improving these models.

Figure 4. Observed (solid arrows) and modelled (blank arrows) displacements of PGGA stations during the Landers/Big Bear earthquakes, shown with 95% confidence ellipses. The contours are for the displacement magnitude based on an elastic half-space model fit to measured near-field displacements and the inversion of strong-motion seismic data. Also shown are the estimates obtained from an independent analysis of the PGGA data by Blewitt *et al.* [1993] at JPL. See Bock *et al.* [1993] for details.

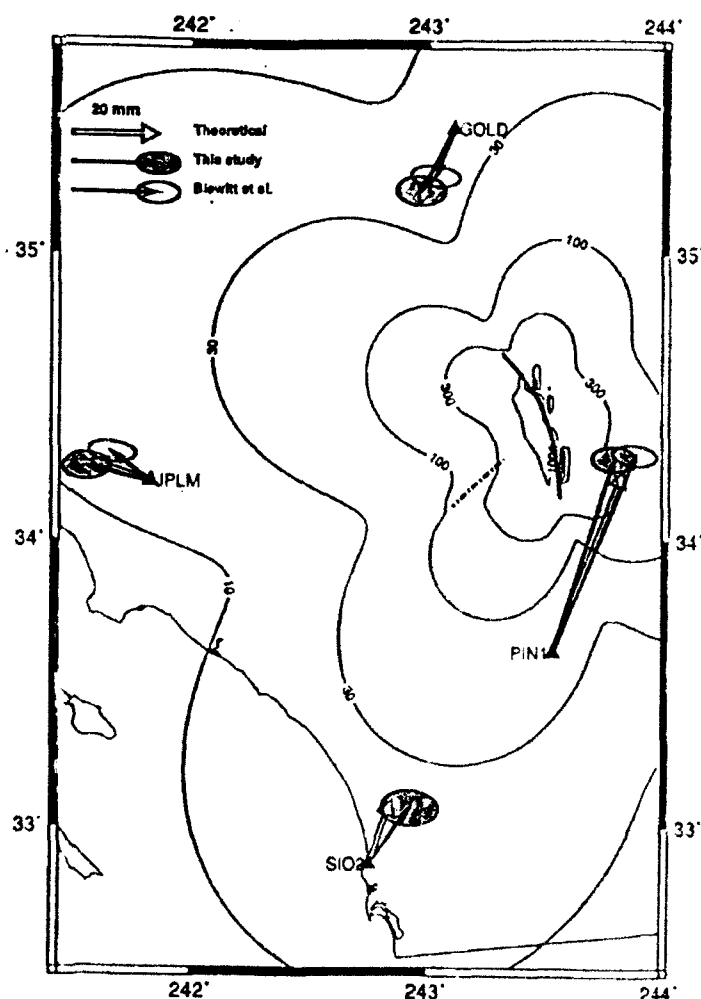
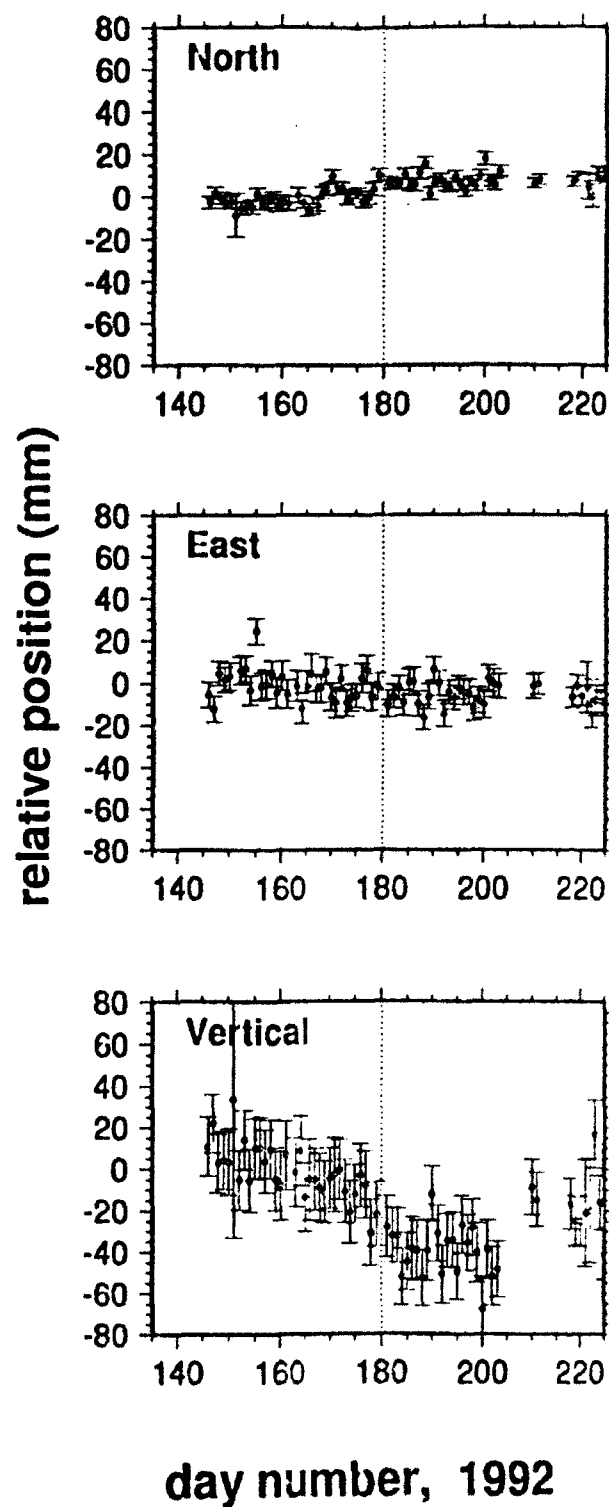


Figure 5. Time series of daily positions of the Vandenberg PGGA antenna with respect to a global reference frame. The error bars represent our best estimate of the one-standard deviation uncertainty of each estimate and have been scaled to account for correlated noise sources. This series may be compared directly with those given in Figure 3 of *Bock et al. [1993]* for other sites in the PGGA.



CITED PUBLICATIONS

- Bock, Y., D. C. Agnew, P. Fang, J. f. Genrich, B. H. Hager, T. A. Herring, K. W. Hudnut, R. W. King, S. Larsen, J.-B. Minster, K. Stark, S. Wdowinski, and F. K. Wyatt, Detection of crustal deformation from the Landers earthquake sequence using continuous geodetic measurements, *Nature*, 361, 337-340, 1993.
- Clark, M. M., K. K. Harms, J. J. Lienkaemper, D. S. Harwood, K. R. Lajoie, J. C. Matti, J. A. Perkins, M. J. Rymer, A. M. Sarna-Wojcicki, R. V. Sharp, J. D. Sims, J. C. Tinsley III, and J. I. Ziony, Preliminary slip-rate table and map of the late Quaternary faults of California, *U. S. Geol. Surv., Open file report 84-106*, 1984.
- Feigl, K. L., R. W. King, and T. H. Jordan, Geodetic measurement of tectonic deformation in the Santa Maria Fold and Thrust Belt, California, *J. Geophys. Res.*, 95, 2679-2699, 1990.
- Feigl, K. L., *Geodetic measurement of tectonic deformation in Central California*, Ph.D. thesis, 222 pp., MIT, Cambridge, MA, 1991.
- Feigl, K. L., D. C. Agnew, Y. Bock, D. Dong, A. Donnellan, B. H. Hager, T. A. Herring, D. D. Jackson, T. H. Jordan, R. W. King, S. Larsen, K. M. Larson, M. H. Murray, Z. Shen, and F. H. Webb, Measurement of the velocity field of central and southern California, 1984-1992, submitted to *J. Geophys. Res.*, December, 1992.
- Hail, C. A., Jr. Origin and development of the Lompoc-Santa Maria pull apart basin and its relation to the San Simon-Hosgri strike slip, western California, *Spec. Rep. 137, Calif. Div. Mines and Geol.*, 1978.
- Hall, C. A., Jr., San Luis Obispo tranform fault and middle Miocene rotation of the western Transverse Ranges, California, *J. Geophys. Res.*, 86, 1015-1031, 1981.
- Jennings, C. W., Fault Map of California, Calif. Geol. Map Ser., map 1, Calif. Div. Mines and Geol., 1975.
- Namson, J., and T. L. Davis, Late Cenozoic fold and thrust belt of the southern Coast Ranges and Santa Maria Basin, California, *Am. Assoc. Pet. Geol. Bull.*, 74, 467-492, 1990.
- Sylvester, A. G., and A. C. Darrow, Structure and neotectonics of the western Santa Ynez fault system in southern California, *Tectonophysics*, 52, 389-405, 1979.

Few of the trends are significant, large surface warming trends are not observed, and like the Western Arctic Ocean analysis in Table 1, significant surface cooling trends are found during winter and autumn. Significant warming trends are observed at the 850 hPa level and the 850–700 hPa layer during winter, in agreement with GCM simulations, but the surface trend is negative. The trends presented in Table 2 are more representative temporally, as they use 36–38 years out of a possible 41, as compared with 20–30 years in the regional analysis (Table 1). On the basis of these tests, we feel that any possible bias introduced by the non-uniform database is small.

The lack of widespread significant warming trends leads us

to conclude that there is no strong evidence to support model simulations of greenhouse warming over the Arctic Ocean for the period 1950–1990. Our results, combined with the inconsistent performance of model simulations of Arctic climate⁶, indicate a need to understand better the physical processes that affect the polar regions, especially atmosphere–ice–ocean interactions, ocean heat transfer and cloud radiative effects, and to incorporate thermodynamic sea ice components into future models. We consider the retrieval of temperature profiles from satellite sounding instruments to be an important means of further resolving the spatial and temporal gradients in Arctic air temperatures. □

Received 23 July, accepted 21 December 1992

- 1 Houghton, J. T. (ed.) *Climate Change: The IPCC Scientific Assessment* (Cambridge Univ. Press, Cambridge, 1990).
- 2 Budko, M. I. *Tellus* **21**, 611–619 (1969).
- 3 Sellers, W. D. *J. appl. Meteorol.* **8**, 392–400 (1969).
- 4 Ingram, W. J., Wilson, C. A. & Mitchell, F. J. B. *J. geophys. Res.* **94**, 8609–8622 (1989).
- 5 Kelly, P. M., Jones, P. D., Sear, C. B., Cherry, B. S. G. & Tavakol, R. K. *Mon. Weath. Rev.* **110**, 71–83 (1982).
- 6 Hansen, J. & Lebedeff, S. *J. geophys. Res.* **92**, 13345–13372 (1987).
- 7 Hansen, J. et al. *J. geophys. Res.* **93**, 9341–9364 (1988).
- 8 Walsh, J. E. & Crane, R. G. *Geophys. Res. Lett.* **19**, 29–32 (1992).
- 9 Walsh, J. E. & Chapman, W. L. *J. Climate* **3**, 237–250 (1990).
- 10 Angell, J. K. *Mon. Weath. Rev.* **114**, 1922–1930 (1986).
- 11 Angell, J. K. & Korshover, J. *Mon. Weath. Rev.* **111**, 901–921 (1983).
- 12 Karoly, D. J. *Geophys. Res. Lett.* **16**, 465–468 (1989).
- 13 Kahl, J. D. et al. *J. geophys. Res.* (submitted).
- 14 Timerev, A. A. & Egorov, S. A. *Meteorol. Gidrol.* No. 7, 50–56 (1991).

- 15 Nagurny, A. P., Timerev, A. A. & Egorov, S. A. *Akad. Nauk SSSR Dokl.* **319**, 1110–1113 (1991).
- 16 Serreze, M. C., Kahl, J. D. & Schnell, R. C. *J. Climate* **5**, 615–629 (1992).
- 17 Serreze, M. C. et al. *J. geophys. Res.* **97**, 9411–9422 (1992).
- 18 Walsh, J. E. *Mon. Weath. Rev.* **105**, 1527–1535 (1977).
- 19 Kahl, J. D., Serreze, M. C., Shiotani, S., Skory, S. M. & Schnell, R. C. *Bull. Am. met. Soc.* **73**, 1824–1830 (1992).
- 20 Serreze, M. C., Kahl, J. D. & Shiotani, S. *National Snow and Ice Data Center Spec. Rep. No. 2* (CIRES, University of Colorado, 1992).
- 21 Skory, S. M. thesis, Univ. of Wisconsin-Milwaukee (1992).
- 22 Diaconis, P. & Efron, B. *Scient. Am.* **248**, 116–130 (1983).

ACKNOWLEDGEMENTS Portions of this work were sponsored by the NOAA's Climate and Global Change Program, the Electric Power Research Institute, and the NSF Division of Polar Programs. The project was conducted as part of the US–Russia Joint Committee on Cooperation in Environmental Protection, the Influence of Environmental Change on Climate (Working Group VIII). Helpful comments were provided by A. A. Tsonis.

Detection of crustal deformation from the Landers earthquake sequence using continuous geodetic measurements

Yehuda Bock, Duncan C. Agnew, Peng Fang,
Joachim F. Genrich, Bradford H. Hager*,
Thomas A. Herring*, Kenneth W. Hudnutt,
Robert W. King*, Shawn Larsen†, J. Bernard Minster,
Keith Stark, Shimon Wdowinski & Frank K. Wyatt

Institute of Geophysics and Planetary Physics, Scripps Institution of Oceanography, La Jolla, California 92093, USA

* Department of Earth, Atmospheric, and Planetary Sciences,

Massachusetts Institute of Technology, Cambridge

Massachusetts 02139, USA

† US Geological Survey, Pasadena, California 91106, USA

‡ Scientific Software Division, Lawrence Livermore National Laboratory, Livermore, California 94550, USA

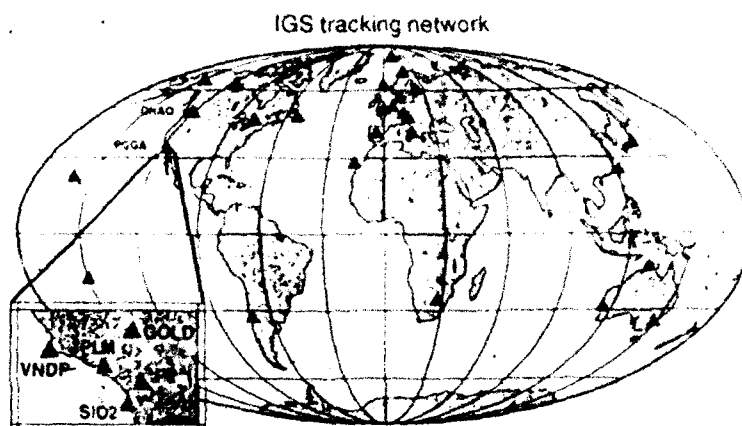
THE measurement of crustal motions in tectonically active regions is being performed increasingly by the satellite-based Global Positioning System (GPS)^{1,2}, which offers considerable advantages over conventional geodetic techniques^{3,4}. Continuously operating GPS arrays with ground-based receivers spaced tens of kilometres apart have been established in central Japan^{5,6} and southern California to monitor the spatial and temporal details of crustal deformation. Here we report the first measurements for a major earthquake by a continuously operating GPS network, the Permanent GPS Geodetic Array (PGGA)^{7–9} in southern California. The Landers (magnitude M_w of 7.3) and Big Bear (M_w 6.2) earthquakes of 28 June 1992 were monitored by daily observations. Ten weeks of measurements, centred on the earthquake events, indicate significant coseismic motion at all PGGA sites, significant post-seismic motion at one site for two weeks after the earthquakes, and no significant preseismic motion. These measurements demonstrate the potential of GPS monitoring for precise detection of

precursory and aftershock seismic deformation in the near and far field.

The PGGA, established in southern California (Fig. 1) in the spring of 1990, is a network of five continuously operating GPS receivers providing an uninterrupted record of crustal motion in near real-time. At each site there is a precise P-code GPS receiver with its antenna mounted on a geodetic monument. Twenty-four hours of data are automatically collected from each site once a day; the operational analysis provides the site position averaged over the day (0–24 h Universal Time Coordinated, UTC), although finer resolution is possible. The precision of the daily relative position between any two sites in the network, based on long-term scatter of nearly 2 years of measurements, is ~5 mm in the horizontal and 10–20 mm in the vertical. To obtain this precision, and to achieve near-real-time solutions, we compute orbits for all GPS satellites, using data collected by a globally distributed network of about 25 permanent tracking stations¹⁰ (Fig. 1), and corrections to tabulated predictions¹¹ of the orientation of the Earth's rotation axis (polar motion). The worldwide tracking network defines a global reference frame in which coordinates for the PGGA stations, in unstable southern California, can be computed with respect to rigid plate interiors (for example, the North American plate).

Here we report measurements of seismically induced displacements of the PGGA stations due to the Landers (M_w 7.3, 11:58 UTC, 34.22° N, 116.43° W) and Big Bear (M_w 6.2, 15:07 UTC, 34.21° N, 116.83° W) earthquakes of 28 June 1992. We examined the series of PGGA station positions in the 10-week period centred on the day of the earthquakes using a Kalman-filter formulation¹² to analyse the daily 24-hour PGGA solutions. For the day of the earthquakes, we computed the station positions separately from the 12 hours of data before the Landers earthquake and the 9 hours of data after the Big Bear event. The global tracking network was fairly extensive as the 3-month International GPS Service campaign¹³ began on 21 June (Fig. 1). Displacements of the PGGA sites, listed in Table 1, were determined by examining the variation in the positions before and after the earthquakes with respect to a global reference frame defined by the coordinates of the tracking network stations. The horizontal displacements of the PGGA sites are

FIG 1 The distribution of global GPS permanent tracking stations and PPGA sites used for our analysis of observations for the period May–August 1992. The closest tracking site outside California is DRAO in Penticton, British Columbia. All stations use Rogue SNR-8 GPS receivers except for two PPGA sites, SIO2 in La Jolla and VNDR at Vandenberg Air Force Base, which use Ashtech LX-113 GPS receivers. The global tracking network is usually described by the acronyms CIGNET and FLINN, standing for Cooperative International GPS Network and Fiducial Laboratories for an International Natural science Network¹⁰, and more recently by the International GPS Service (IGS)^{11,12}.



plotted in Fig. 2. The maximum horizontal displacement of 48 mm was detected at PIN1, located at the Piñon Flat Observatory (PFO) ~80 km from the seismic rupture zone. In Fig. 3 we take differences for the positions obtained with respect to the global reference frame and plot the daily record of relative horizontal positions between PIN1 and three other stations (Fig. 1). These were a global tracking site (DRAO) near Penticton, British Columbia, Canada, more than 1,700 km to the north and the global tracking station closest to the PPGA; the PPGA site (JPLM) in Pasadena; and the PPGA site (GOLD) at the NASA Deep Space Network Goldstone Complex.

An examination of the station displacements indicates that most of the deformation is due to the coseismic phase of the crustal deformation cycle¹⁴. The coseismic displacements appear clearly as step functions in the time series of daily station positions (Fig. 3). No significant pre-seismic signature is discernible from the five weeks of daily data taken before the earthquakes. There appears, however, to be a significant post-

seismic signature of $0.9 \pm 0.3 \text{ mm day}^{-1}$ in our estimates of the relative positions of GOLD and PIN1 for 16 days after the earthquakes (Fig. 3). An examination of the displacements at the individual stations indicates that most of the post-seismic motion occurs at GOLD at a rate of $0.7 \pm 0.3 \text{ mm day}^{-1}$. (We were concerned that displacements observed at GOLD might stem from the construction of its antenna support, a 12-m-high microwave tower. This station, unlike the other PPGA stations which have very stable geodetic monuments, was neither installed nor operated primarily for monitoring tectonic motions, and might easily be recovering from the mainshock accelerations. Comparing the changing position of this monument with respect to another continuously operating GPS receiver 10 km away indicates, however, that the displacements were tectonic in origin.) The remainder of the motion, ~3 mm in total, occurs at PIN1, but the rate of displacement is not well determined from the data. Greater temporal detail and higher short-term resolution is provided by laser strainmeters at PFO; these show no pre-seismic signal, although post-seismic slip in the first 1–2 weeks following the earthquakes are consistent with our observations at PIN1. Further discrimination of the post seismic signal will require the implementation of more refined analysis techniques. We intend to study the much longer time series of data before and after the earthquakes to look for possible pre-seismic signals and changes in the interseismic rate of deformation, and to understand better the error spectrum of continuous GPS data. We are currently investigating an increase in

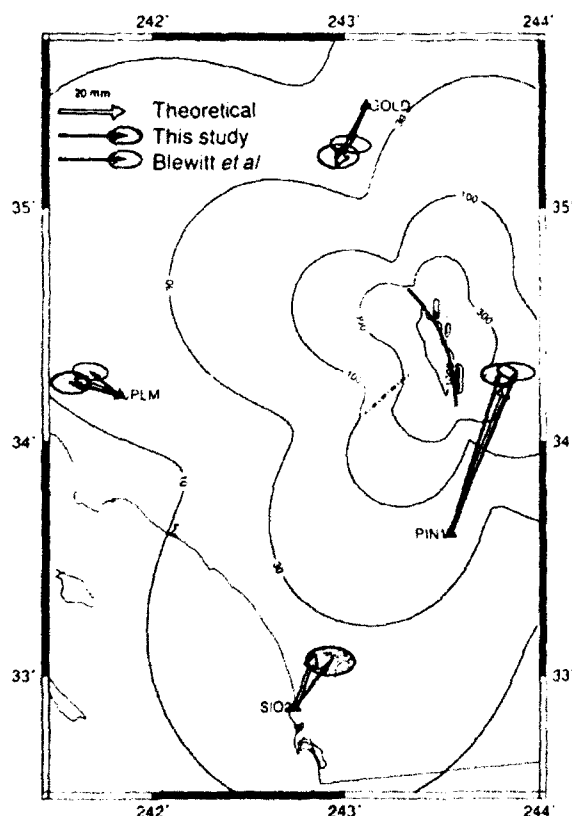


FIG 2 Observed (solid arrows) and modelled (blank arrows) displacements at the PPGA stations including 95% confidence ellipses. The observed displacements are calculated with respect to the reference frame defined by the positions and velocities of the global tracking stations, and include the total displacement estimated over the 5-week period after the earthquakes. Except for GOLD and a very small effect at PIN1, the displacements seem to be due entirely to coseismic motion. The total displacement observed at GOLD is 17 mm which includes ~6 mm of coseismic motion and 11 mm of apparent post-seismic motion over the 16 days following the earthquakes. For comparison we show the displacements and 95% confidence ellipses (unshaded) computed by Blewitt *et al.*¹⁵. The contours of displacement magnitude, and the calculated displacements are for an elastic halfspace (all units are millimetres). The surface trace of the Landers rupture (heavy line) is composed of six segments with end points at latitude and longitude (degrees) (34.1500, 243.5708), (34.2250, 243.5625), (34.3625, 243.5375), (34.4500, 243.5000), (34.4958, 243.4750), (34.5917, 243.3917) and (34.6542, 243.3208). The magnitudes of slip are 1.5, 3.5, 1.0, 4.8, 5.2 and 0.8 m right-lateral respectively, with all segments from 0 to 15 km depth. The dashed line shows the surface trace assumed for the fault segment of the Big Bear earthquake, with 0.4 m of left-lateral slip on a segment from 3 to 15 km depth, and end points (34.1200, 243.1037) and (34.2884, 243.3297).

TABLE 1 Theoretical and observed displacements

Site	Distance (km)	North (mm)		East (mm)		Amplitude (mm)			Azimuth (deg)		Vertical (mm)	
		M	O	M	O	M	O	M:O	M	O	M	O
PIN1	89	42.8	45.6 ± 1.2	16.2	14.0 ± 2.1	45.8	47.7 ± 2.4	0.96	20.7	17.1	3.6	13.8
GOLD	117	-17.5	-14.6 ± 1.4	-8.5	-8.0 ± 2.4	19.5	16.6 ± 2.8	1.17	205.9	208.7	-2.8	7.3
JPLM	155	4.7	3.4 ± 1.3	-13.4	-14.7 ± 2.4	14.2	15.1 ± 2.7	0.94	289.3	283.0	6.3	0
SIO2	185	15.1	13.0 ± 1.7	6.0	10.1 ± 2.8	16.2	16.5 ± 3.3	0.98	21.7	37.8	-16.1	8.9
VNDP	380	0.9	4.5 ± 1.6	-3.0	-4.1 ± 2.5	3.1	6.1 ± 3.0	0.51	286.7	317.7	-31.0	2.6

Total displacements in the horizontal components of the PGGA stations computed by a variable slip dislocation model (M) and estimated from 10 weeks of GPS observations (O) centred on the day of the earthquakes, and a comparison of the modelled and observed amplitudes and azimuths of the displacements. The displacements are computed with respect to the global reference frame defined by the global tracking stations (Fig. 1). The errors listed for the observed displacements are 1σ values. The distance from the PGGA sites to the centroid of the model is given. For completeness we include the vertical displacements computed from the dislocation model and estimated from the GPS observations. In this case, the table gives the values for the motion of the PGGA sites relative to JPLM which has been shifted to 0 for both observation and model values. This requires adding 3.7 mm to the model value and 25.9 mm to the observed value. The vertical component errors are not well understood, however, so the agreement with the dislocation model may be fortuitous.

the data noise after the earthquakes (Fig. 3); this may partly be a meteorological effect related to the transition into summer, a phenomenon that has been observed in many years of positions determined by very-long-baseline interferometry in California.

An independent analysis of the PGGA and global tracking data by a group at the Jet Propulsion Laboratory (JPL) yielded

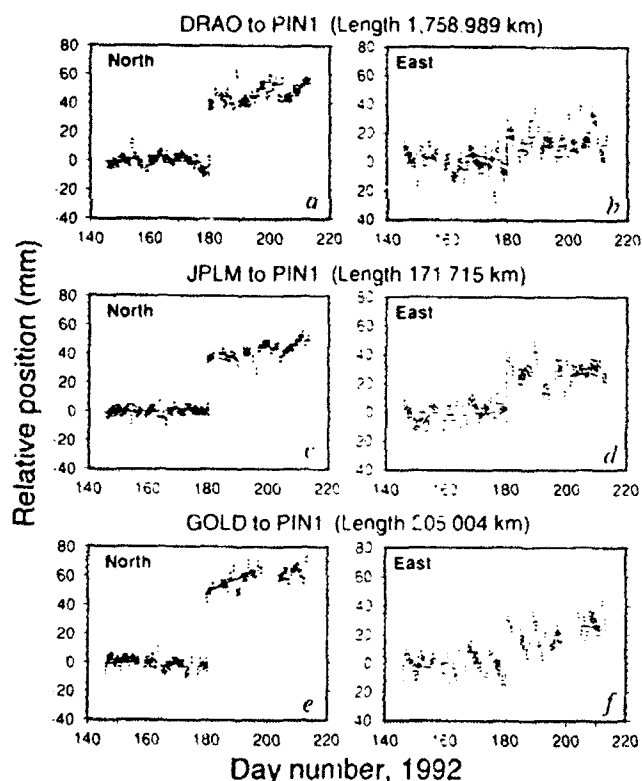


FIG. 3 Time series of daily horizontal relative positions (north and east components) over a 10-week period centred on the day of the earthquakes (day 180, 28 June 1992) for PIN1 relative to DRAO (a, b), JPLM (c, d) and GOLD (e, f). The dotted horizontal lines are determined from the weighted means of the data for the 5-week period before and after the earthquakes, and indicate the coseismic signature (these differ from the Kalman-filter estimates given in Table 1 by not more than 2.5 mm). The error bars have been scaled by a factor of two to account for the effects of correlated noise sources. These are not included in our statistical estimates of the uncertainties, which assume white-noise error sources. In e we fit by least squares a straight line, with a slope of 0.9 ± 0.3 mm day⁻¹, to the apparent post-seismic signature for the 16 days following the earthquakes. The east component has a larger scatter than the north component because the integer-cycle phase ambiguities were not resolved to integer values^{16,18} in the daily PGGA solutions.

similar total displacements, as reported by Blewitt *et al.*¹⁵. The JPL group used the GIPSY GPS software^{16,17} to process the data whereas we used the GAMIT/GLOBK GPS software^{12,18}. The algorithms used in these two programs were independently developed and use different approaches. Furthermore, the two groups used different global reference frames and different subsets of the global tracking and PGGA data. We analysed ten weeks of data from all five PGGA sites, which included three Rogue SNR-8 GPS receivers and two Ashtech LX-II3 GPS receivers (at VNDP and SIO2), whereas Blewitt *et al.* analysed 8 weeks of Rogue receiver data only. A comparison of the results is shown in Fig. 2. The overlaps of our respective 95% confidence ellipses indicate good agreement at the three common sites.

In Fig. 2 we show the coseismic displacements computed from a variable slip dislocation model in an elastic halfspace^{19,20}. The model for the Landers earthquake separates the 65-km rupture into six vertical planar segments (Fig. 2), oriented to coincide with the epicentre and the curvilinear pattern observed in the surface break and aftershock distribution²¹. The right-lateral slip on the southernmost three segments was calculated by averaging over each segment the observed surface offset and the slip distribution obtained by inverting strong-motion seismic data²². Slip on the northern three segments was obtained by fitting the displacement vector at GOLD. This required significantly less slip than observed along the surface break. The surface faulting observed geologically continued 10 km to the northwest of the main aftershock zone, suggesting that rupture along this segment of the fault is confined to shallow depths^{15,21}. The Big Bear event was modelled as left-lateral rupture along a vertically dipping fault, oriented to coincide with the focal mechanism and aftershock distribution; the slip was chosen to agree with the seismic moment (H. Kanamori, personal communication).

There is good agreement between the theoretical and observed displacements at the PGGA sites (Table 1, Fig. 2). Our fit to the displacement vectors, although nonunique, suggests less slip in the northern half of the Landers rupture. In fact, the geodetic moment calculated using these far-field PGGA data is 0.8×10^{20} N m, which is generally less than moments obtained by independent means: near-field seismic (0.8 – 0.9×10^{20} N m), geological (0.9×10^{20} N m), near-field geodetic (1.0×10^{20} N m) and teleseismic (1.1×10^{20} N m)^{21,23}. The comparatively low PGGA moment may be a manifestation of the influence of the mantle, which has higher values of elastic moduli than the crust²⁴, so that far-field amplitudes of theoretically computed displacements are reduced relative to homogeneous halfspace models. In this case, the far-field is distances greater than the 30 km thickness of the crust.

These data show that continuous GPS arrays can provide reliable, precise and rapid determination of crustal motion, in particular seismically induced deformation. Although dense spatial coverage with such stations is not economically feasible

at present, advances in GPS receiver technology will allow denser and more continuous measurements.

Received 17 August; accepted 11 December 1992

1. Dixon T. H. *Rev. Geophys.* **29**, 249–276 (1991).
2. Hager B. H., King R. W. & Murray M. H. *Rev. Earth planet. Sci.* **19**, 351–382 (1991).
3. Sauber J., Thatcher W. & Solomon S. C. *J. geophys. Res.* **93**, 12683–12693 (1988).
4. Savage J. *Geophys. Res. Lett.* **17**, 2113–2116 (1990).
5. Shimada S. *et al. Nature* **343**, 631–633 (1990).
6. Shimada S. & Bock Y. *J. geophys. Res.* **97**, 12437–12455 (1992).
7. Bock Y. & Leppard N. (eds) *Global Positioning System An Overview* 40–56 (Springer, New York, 1990).
8. Lindqvist U., Blewitt G., Zumbeke J. & Webb F. *Geophys. Res. Lett.* **18**, 1135–1138 (1991).
9. Bock Y. *GPS World* (Aster, Eugene, Oregon, 1991).
10. Minster J. B., Hager B. H., Prescott W. H. & Schultz R. E. *International Global Network of Fiducial Stations* (National Res. Council, National Academy Press, Washington DC, 1991).
11. International Earth Rotation Service. *Bulletins B 51–54* (Observatoire de Paris, 1992). *Bulletins A Vol. V* (US Naval Observatory, 1992).
12. Herring, T. H., Davis J. L. & Shapiro J. I. *J. geophys. Res.* **95**, 12561–12583 (1990).
13. Beutler, G. *Eos* **73**, 134 (1992).
14. Scholz, C. H. *The Mechanics of Earthquakes and Faulting* (Cambridge Univ. Press, 1990).
15. Blewitt G. *et al. Nature* **361**, 340–342 (1993).
16. Blewitt G. *J. geophys. Res.* **94**, 10187–10203 (1989).
17. Blewitt G. *Geophys. Res. Lett.* **17**, 199–202 (1990).
18. Dong, D. & Bock Y. *J. geophys. Res.* **94**, 3949–3966 (1989).
19. Mansinha L. & Smylie, R. E. *Bull. seism. Soc. Am.* **61**, 1433–1440 (1971).
20. Okada, Y. *Bull. seism. Soc. Am.* **75**, 1135–1154 (1985).
21. Landers Earthquake Response Team Science (submitted).
22. Kanamori, H., Thio H.-K., Dreger D., Hauksson, E. & Heaton T. *Geophys. Res. Lett.* **19**, 2267–2270 (1992).
23. Hudnut, K. W. *et al. Eos* **73**, 365 (1992).
24. Rybicki, K. *Bull. Seism. Soc. Am.* **61**, 79 (1971).

ACKNOWLEDGEMENTS We thank K. Feigl and J. Savage for reviews. H. Kanamori for assistance our colleagues at JPL, especially S. Dinardo for maintaining the quality of the PGGA and much of the global tracking network, and G. Blewitt for assistance in comparing results. We thank the US National Geodetic Survey and Energy Mines and Resources Canada and the participants in the International GPS campaign (IGS) for data and resources. Supported by NASA, NSF, the Southern California Earthquake Center, the US Geological Survey and the US Air Force Office of Scientific Research. S.L.'s work was done under the auspices of the US Dept. of Energy by the Lawrence Livermore National Laboratory. Y.B.'s work was done in part through a Scripps/JPL joint appointment.

Absolute far-field displacements from the 28 June 1992 Landers earthquake sequence

Geoffrey Blewitt, Michael B. Heflin, Kenneth J. Hurst, David C. Jefferson, Frank H. Webb & James F. Zumbeke

Jet Propulsion Laboratory, California Institute of Technology, Pasadena California 91109, USA

ON 28 June 1992, the largest earthquake in California in 40 years (surface-wave magnitude $M_s = 7.5$) occurred near the small town of Landers, in southeastern California, and was followed three hours later by the nearby M_s 6.5 Big Bear earthquake¹. Fortunately, the Landers earthquake sequence coincided with the first week of the official three-month test period of the International Global Positioning System and Geodynamics Service² (IGS), giving us an unprecedented opportunity to detect absolute pre-, co- and post-seismic displacements at a distance of 50–200 km from the main rupture with millimetre-level precision. Mutual and independent confirmation of some of our geodetic results are demonstrated by Bock *et al.* in this issue³. For the Landers earthquake, the observed displacements indicate that the depth of the bottom of the rupture is shallower towards the northern end, displacements were dominantly symmetric, and the rupture extended further south on the Johnson Valley fault than has been mapped on the basis of surface ground offsets. The combined geodetic moment for the Landers and Big Bear earthquakes (1.1×10^{20} N m⁻¹) agrees well with teleseismic estimates.

The Landers and Big Bear earthquakes and their aftershocks occurred along faults that form a triangle bounded to the southwest by the San Andreas fault (Fig. 1). Extensive surface rupture resulting from these events has been reported along the Johnson

Valley and Camp Rock/Emerson faults. Ground breakage occurs along a 70-km stretch of these faults, reaching a maximum surface offset of 6.7 m (ref. 1). The Landers earthquake occurred toward the southern end of the hypothesized 'Mojave shear zone', which trends N35°W across the Mojave Desert, into Owens Valley and the northern Basin and Range province^{4,5}. This zone reportedly carries 7–8 mm yr⁻¹ of the relative motion between the Pacific and North American plates, and may be a manifestation of a subcrustal fault^{4,5}. Aftershocks following the Landers earthquake line up along this apparent shear zone from as far south as the San Andreas fault, to further north than our station GOLD shown in Fig. 1. The pattern of aftershocks is sparse on the Camp Rock fault segment which underlies the northernmost 13 km of the visible surface rupture⁶. Using a new geodetic tool for earthquake studies, we have estimated permanent surface displacements in southern California due to the cumulative effect of events on 28 June, and show that geodetic methods provide valuable information on aspects of the rupture mechanism not available with other techniques. We also offer an explanation for the unexpected lack of aftershocks on the Camp Rock fault.

Since 21 June 1992, a worldwide network of stations has been routinely receiving precise microwave ranging data from the United States Department of Defence's 18-satellite Global Positioning System (GPS)⁷, and transmitting the data to IGS data centres to be made available to analysis centres and geodynamics researchers. Regional GPS networks benefit from the precise orbit determination and reference frame stability supplied by an extensive tracking network^{8–10}. A regional array of receivers operated jointly by the Jet Propulsion Laboratory (JPL) and Scripps Institution of Oceanography has been operational in southern California since 1990 (ref. 11). A simultaneous analysis of GPS data from the California array combined with the global network data has allowed us to estimate the absolute displacements, in the international terrestrial reference frame¹² (ITRF), of three stations located within 50–200 km from the Landers earthquake rupture, with 2-mm precision in the horizontal plane.

To reduce systematic errors that can be introduced by mixing different types of GPS receivers and antennas, we have analysed

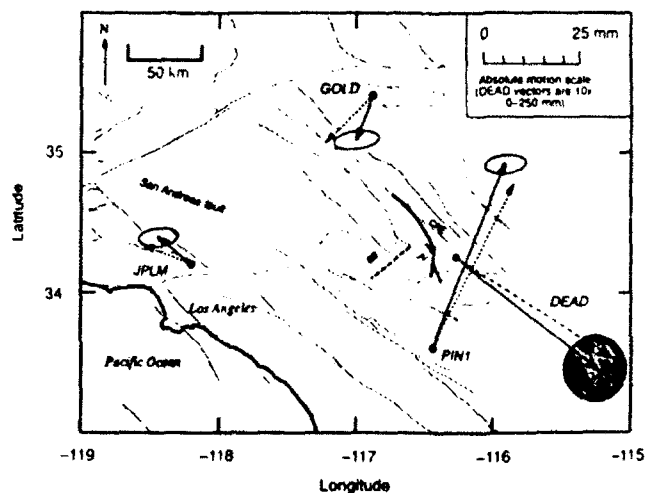


FIG. 1 Map showing absolute motions of Goldstore (GOLD), Pasadena (JPLM), Pinyon Flat (PIN1) and Deadman (DEAD). Solid arrows are the observed displacements with 95% confidence regions. The vectors and confidence region for DEAD is shown at 0.1 times the scale of the other stations. The model displacements, assuming an elastic half-space, are shown as dashed arrows. The surface trace of the model of the Landers earthquake is shown by the solid heavy line. Dashed heavy line (BB) is the trace of the fault used to model the Big Bear earthquake. Shaded solid and dashed lines are active faults in the region. JV is the Johnson Valley fault; CRE is the Camp Rock/Emerson fault.